

Determining salinization extent, identifying salinity sources, and estimating chloride mass using surface, borehole, and airborne electromagnetic induction methods

Jeffrey G. Paine

Bureau of Economic Geology, John A. and Katherine G. Jackson School of Geosciences
University of Texas at Austin, Austin, Texas, USA

Received 7 July 2001; revised 6 July 2002; accepted 6 July 2002; published 19 March 2003.

[1] Using an example from an oil field in the semiarid Red River basin in Texas, we show that electromagnetic (EM) methods are useful in locating salinized soil and water, determining salinization extent, identifying likely salinity sources, and estimating the total mass of chloride within a saline-water plume. Each of these aspects assists in managing salinization and assessing its impact. We used ground EM instruments to establish salinization boundaries and determine the range of electrical conductivity, airborne measurements to locate potential sources and quantify the lateral extent and intensity of salinization, and borehole measurements and time domain EM soundings to determine salinization depth and relate ground conductivity to chloride content. We estimated infiltration volume and total chloride mass in the plume from EM data and an empirical, site-specific chloride:conductivity ratio established from well data. Because the measured conductivity of water strongly correlates with total dissolved solids concentration, mass estimation could be extended to any ionic constituent that covaries linearly with total dissolved solids concentration. EM methods owe their success to the large increase in electrical conductivity that occurs where highly conductive, saline water infiltrates geologic materials having naturally low conductivities. *INDEX TERMS:* 0694

Electromagnetics: Instrumentation and techniques; 1831 Hydrology: Groundwater quality; 1894 Hydrology: Instruments and techniques; *KEYWORDS:* salinization, electromagnetic induction, airborne geophysics, total dissolved solids, produced water, brine

Citation: Paine, J. G., Determining salinization extent, identifying salinity sources, and estimating chloride mass using surface, borehole, and airborne electromagnetic induction methods, *Water Resour. Res.*, 39(3), 1059, doi:10.1029/2001WR000710, 2003.

1. Introduction

[2] Salinization of soil and water is a common problem in arid and semiarid regions around the world [Ghassemi *et al.*, 1995]; its impact is felt in many population centers and agricultural provinces. Examples abound from Australia [Macumber, 1969; Hillman, 1981; Schofield and Ruprecht, 1989], the Middle East [Rosenthal *et al.*, 1992; Vengosh and Ben-Zvi, 1994; Marie and Vengosh, 2001], Africa [Kirchner *et al.*, 1997; Valenza *et al.*, 2000], Asia [Smith, 1992; Chen *et al.*, 1997; Funakawa *et al.*, 2000; Wang *et al.*, 2000], South America [Gilboa, 1977], North America [Nightingale, 1974; Miller *et al.*, 1981; Dutton *et al.*, 1989; Hendry and Buckland, 1990; Richter and Kreitler, 1993], and India [Prakash and Chadha, 1983]. Soil salinization diminishes crop yields, increases runoff and soil erosion, and contributes to desertification [Banin and Fish, 1995]. Water salinization degrades surface water and groundwater supplies, limits irrigation, requires treatment for municipal and industrial uses, perturbs riverine ecosystems, causes freshwater plants to be replaced by salt-tolerant ones, and affects recreational and commercial fisheries.

[3] Major potential causes of near-surface salinization include (1) migration of subsurface saline water through faults, fractures, or permeable geologic units where driven by gravity or fluid pressure; (2) intrusion of seawater in coastal areas; (3) evaporative concentration of groundwater from shallow water tables that have risen in response to irrigation, landscaping, or vegetation alteration; (4) infiltration of oil field brine beneath surface disposal pits and through leaking oil and gas wells; and (5) road salting [Kovda, 1946; Barica, 1972; Richter *et al.*, 1990; Richter and Kreitler, 1993; Ghassemi *et al.*, 1995].

[4] Remote sensing methods, including analysis of aerial photographic and satellite images [Johnston and Kamprad, 1988; Dwivedi *et al.*, 1999; Pankova and Rukhovich, 1999], have been used to detect salinization but may underestimate its lateral extent beneath unaffected vegetation. Geochemical methods [Whittemore, 1984, 1995; Dutton *et al.*, 1989; Richter and Kreitler, 1993] have been developed to distinguish salinity sources but commonly require extensive soil, surface water, and groundwater sampling and chemical analyses.

[5] Geophysical methods, particularly electromagnetic (EM) induction, complement remote sensing and geochemical approaches. EM methods have proven to be very effective in locating salinized areas, mapping the extent and intensity of salinization, and locating potential salinity

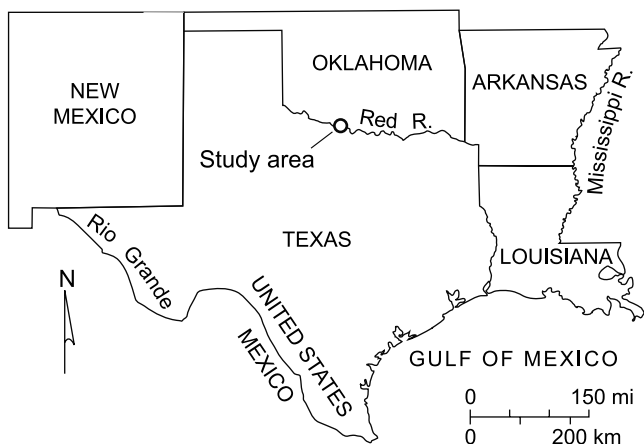


Figure 1. Location of the study area within the Red River drainage basin, Montague County, Texas.

sources in support of more invasive studies. Early geophysical instruments used to estimate soil salinity indirectly included in situ transducers and electrode arrays to measure soil conductivity [Enfield and Evans, 1969; Halvorson and Rhoades, 1974]. During the late 1970s and early 1980s, investigators began developing and using EM instruments to measure ground conductivity noninvasively and estimate soil and water salinity at depths ranging from less than 1 to more than 50 m [De Jong *et al.*, 1979; McNeill, 1980a, 1980b; Rhoades and Corwin, 1981; Corwin and Rhoades, 1982, 1984; Williams and Baker, 1982; Williams and Braunach, 1984; Williams and Fidler, 1985]. Statistical techniques have been developed to predict soil salinity and monitor temporal changes by combining EM and soil sampling [Lesch *et al.*, 1995, 1998]. Ground-based EM methods continue to be used widely in salinity mapping [McKenzie *et al.*, 1997; Banerjee *et al.*, 1998]. The EM method is popular because it can be rapidly and noninvasively applied. It is effective because a large increase in electrical conductivity typically accompanies the introduction of extremely conductive saline water (several hundred to several thousand millisiemens per meter [Hem, 1985]) into freshwater, soil, and rock that generally have low natural conductivities (a few tens to a few hundred millisiemens per meter [McNeill, 1980a]).

[6] This paper illustrates how we combined several EM methods to assess near-surface salinization within a 35 km² area along the Red River in Montague County, Texas (Figure 1). In this semiarid environment an area barren of vegetation formed on a cultivated Pleistocene alluvial terrace in the 1980s and expanded during the 1990s to encompass 219,000 m² on the terrace [Hovorka *et al.*, 1999a, 1999b]. The terrace lies topographically below and adjacent to an oil field on the Permian upland (Figure 2) that has been operating since the 1920s, has produced brine along with hydrocarbons, and has had some of the produced brine discharged onto the surface and into pits before Texas's no-pit order was implemented by the Railroad Commission of Texas in 1969. Depths to the relatively shallow water table range from 4 to 10 m on the upland and less than 2–6 m on the terrace. We used surface, borehole, and airborne EM methods to (1) establish lateral and vertical extent of salinization, (2) map the degree of

salinization, and (3) identify potential salinity sources in a large saline-water plume associated with the barren area. We combined this information with chemical data from water samples to estimate chloride mass within the plume, assess the plume's potential impact on the Red River, and evaluate remediation options.

2. Methods

[7] We used frequency and time domain EM methods to measure apparent electrical conductivity to depths of 50–100 m in the study area. Frequency domain EM methods use a changing primary magnetic field created around a transmitter coil to induce current to flow in the ground or in the annulus around a borehole, which in turn creates a secondary magnetic field that is sensed by the receiver coil [Parasnis, 1973; Frischknecht *et al.*, 1991; West and Macnae, 1991]. The strength of the secondary field is a complex function of EM frequency and ground conductivity [McNeill, 1980b] but generally increases with ground conductivity at constant frequency. Time domain EM (TDEM) devices measure the decay of a transient, secondary magnetic field produced by currents induced to flow in the ground by the termination of a primary electric current [Kaufman and Keller, 1983; Spies and Frischknecht, 1991] flowing in a transmitter loop. The secondary field strength is measured by the receiving coil at discrete time intervals following transmitter current termination. In horizontally layered media, secondary field strength at early times gives information on conductivity in the shallow subsurface; field strength at later times is influenced by conductivity at depth.

[8] Geophysical investigations consisted of ground-based-reconnaissance, high-resolution-airborne, and follow-up borehole and TDEM surveys. Reconnaissance surveys were completed using the Geonics EM34-3 ground conductivity meter that was chosen on the basis of expected salinization to depths of a few tens of meters. We used this instrument to establish the range of conductivity values, the lateral salinization boundaries, and the presence of multiple salinity sources represented as local conductivity peaks. On the basis of reconnaissance results, boundaries and acquisition parameters were chosen for the airborne EM survey. Airborne, frequency domain EM data were acquired in 1997 by Geotrex-Dighem (now Fugro Airborne Surveys) using helicopter-borne horizontal coplanar coils operating at 900, 7200, and 56,000 Hz and vertical coaxial coils operating at 900 and 5500 Hz at an instrument height of 30 m and a flight-line spacing of 100 m over the 35 km² study area. Geotrex-Dighem processed the airborne data, calculating apparent half-space conductivities for each coplanar coil frequency at each measurement point. Measurement spacing along each flight line was 3 m, providing the high-resolution coverage needed to identify salinity sources and quantify salinized areas accurately. Similar airborne surveys have been completed in Mississippi [Smith *et al.*, 1997] and west Texas [Paine *et al.*, 1997, 1999] to locate conductivity and magnetic field anomalies associated with oil field salinity sources that include brine-disposal pits, surface spills, and leaking wells.

[9] At the Montague County site, patterns evident on apparent ground conductivity maps produced from the airborne data guided borehole placement and follow-up studies that included TDEM soundings, borehole logging, and water sampling. We acquired TDEM soundings at the

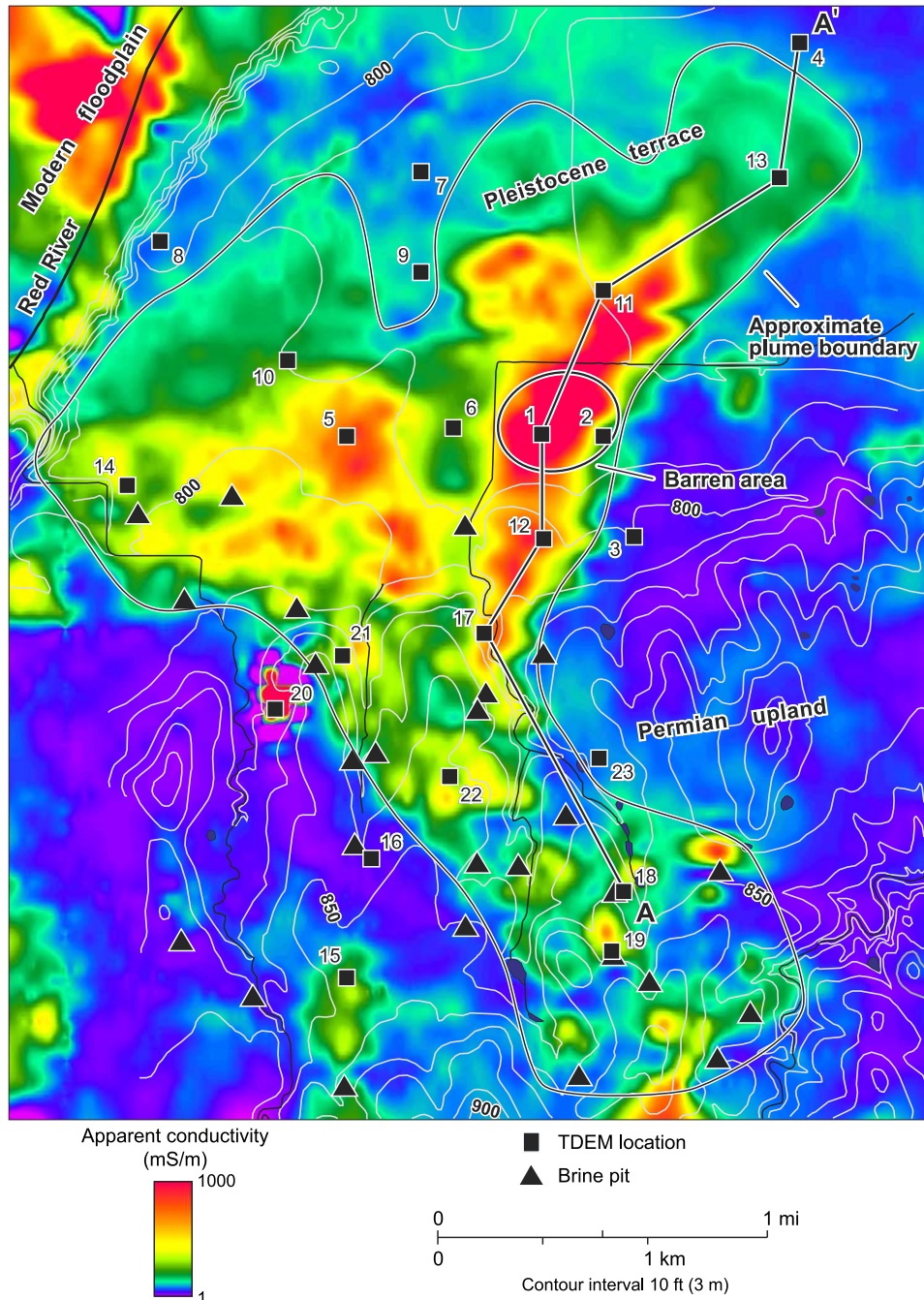


Figure 2. Topographic map of the study area superimposed on apparent conductivity measured using 7200 Hz airborne induction coils. The Permian upland, the high-relief area occupying the southern half of the map, includes part of the Nocona North Oil Field. Approximate boundaries of the oil field are defined by former pit locations determined from 1966 aerial photographs. A Pleistocene terrace (low relief) covers most of the northern part of the map between the modern Red River floodplain and the Permian upland.

surface using a Geonics Protem 47 instrument. We used the computer program TEMIX, by Interpex, to construct model conductivity profiles that produce synthetic transients that match the observed transients. To acquire a sounding, a 40×40 m, single-wire transmitter loop carrying an alternating current of 2 A was placed on the ground. We then placed a receiver coil at the center of the transmitter loop and recorded the transient signal between $7 \mu\text{s}$ and 2.8 ms after current cutoff. Exploration depth was 50–100 m.

TDEM soundings established the thickness of the saline-water plume, and borehole EM logs verified the relationship between lithologic units, chloride content, and measured electrical conductivity.

3. Results

[10] Reconnaissance measurements revealed that apparent conductivities ranged from less than 50 mS m^{-1} in

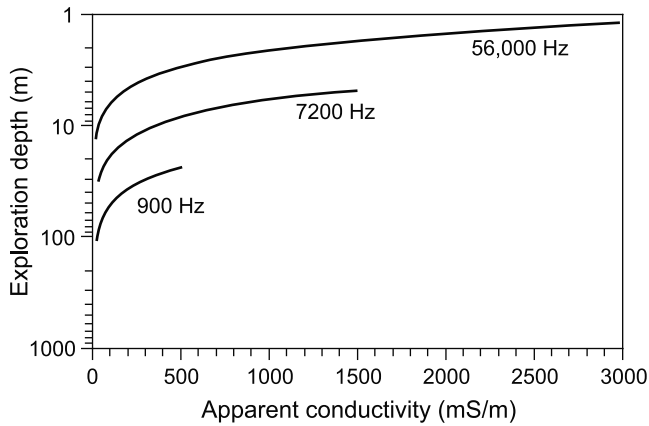


Figure 3. Changes in exploration depth (skin depth) with ground conductivity for 900, 7200, and 56,000 Hz airborne coil configurations. Line ranges correspond to conductivity ranges observed in the study area.

areas having no evidence of salinization to 200 mS m^{-1} or more across saltwater seeps and barren areas. These surveys also indicated that (1) there is a conductivity anomaly associated with the barren area on the Pleistocene terrace; (2) the conductivity anomaly underlies an area that is much larger than the barren area; (3) several local conductivity anomalies exist along the drainages that cross the oil field, suggesting more than one source of saline water; and (4) the salinity sources and salinization are bounded by an area that is about 5 km east-west by about 7 km north-south (Figure 2). This area was subsequently surveyed using airborne instruments.

[11] Maps of apparent ground conductivity, as measured by the airborne 56,000, 7200, and 900 Hz induction coils, are similar; each clearly shows the extent of highly conductive ground associated with the saline-water plume (Figure 2). Exploration (skin) depth, defined as the depth at which the primary field strength is reduced to $1/e$ times its original value, depends on both the conductivity of the ground and the frequency of the instrument. Skin depth is calculated using the equation

$$d = k(\rho/f)^{0.5},$$

where d = skin depth (in meters), $k = 500 \text{ (m/ohm-s)}^{0.5}$, ρ = resistivity (in ohm-m), and f = EM frequency (in cycles s^{-1}) [Telford *et al.*, 1976]. Recast into equivalent, reciprocal conductivity terms, this equation becomes

$$d = k(1/\sigma f)^{0.5},$$

where $k = 15,681 \text{ (m-mS s}^{-1})^{0.5}$, σ = conductivity (in mS m^{-1}), and f = EM frequency.

[12] Exploration depths for the 56,000 Hz coils, calculated from the known frequency and from the observed apparent conductivity range of $25\text{--}3000 \text{ mS m}^{-1}$, increase from about 1 m for the most conductive ground to about 14 m for the least conductive ground (Figure 3). Apparent conductivities measured by the 7200 Hz coils, ranging from 25 to 1500 mS m^{-1} (Figures 2 and 3), are lower than those

measured by the 56,000 Hz coils. Exploration depths for this frequency are between 5 and 38 m, decreasing with increasing conductivity. At 900 Hz, airborne coils measured apparent conductivities that ranged from 25 to 500 mS m^{-1} . Exploration depths for this frequency are between 25 m for the most conductive ground to more than 75 m for the least conductive ground.

[13] Particularly at the two higher frequencies, many conductivity anomalies in the oil field on the Permian upland coincide with known brine-pit locations visible on aerial photographs taken in 1966 before pit closure (Figure 2). Each of these anomalies is several hundred meters across. As exploration depth increases, the degree of connection between adjacent anomalies and with the large anomaly on the Pleistocene terrace increases, suggesting that discharge of produced brine into the pits was a major source of saline water. The $219,000 \text{ m}^2$ barren area on the Pleistocene terrace falls within a much larger conductivity anomaly that underlies about 10 km^2 and has apparent conductivities ranging from just above background values (about 50 mS m^{-1}) to the highest conductivities observed for each frequency (Figure 2). This large anomaly has a sharp eastern boundary that may be controlled by paleotopography on the buried Permian surface, a bifurcation into a northeast trending branch and a west trending branch, and a diffuse northern boundary. Parts of the modern floodplain of the Red River, and the river itself, are also highly conductive, reflecting the high chloride concentrations in the river and its alluvium attributed to upstream natural and anthropogenic sources [Red River Authority of Texas, 1996]. The low elevation of the river and its modern alluvium and observed groundwater flow directions eliminate the river as a potential source of the saline water on the higher Permian upland and Pleistocene alluvial terrace (Figure 2). Saline seeps along the base of the Pleistocene terrace demonstrate flow from the plume to the modern floodplain and river itself.

[14] Much as results from the ground-based surveys were used to design the airborne survey, results from the airborne survey were used to determine optimal borehole locations and follow-up geophysical sites. Borehole induction logs (Figure 4) and chemical analyses of water samples from monitoring wells verified that the large conductivity anomaly on the Pleistocene terrace is caused by high total dissolved solids (TDS) concentrations in near-surface deposits below the water table and that the salinity signature is consistent with that of brine produced from the adjacent oil field [Hovorka *et al.*, 1999a].

[15] It is possible to invert airborne EM data to obtain estimates of changes in subsurface conductivity with depth, but the accuracy of these depth inversions may be limited by the small number of measurements at each point. Better vertical resolution can be obtained using borehole instruments or, to a lesser degree, ground TDEM instruments. We acquired borehole logs in 16 monitoring wells within and outside the plume and supplementary TDEM soundings at 23 sites on the Permian upland and Pleistocene terrace (Figure 2) to obtain generalized conductivity profiles with depth and to estimate depth of salinization. Transient signatures from TDEM soundings in saline-water plume and nonplume locations clearly differ (Figure 5). Transients measured in nonplume areas have short durations (less than

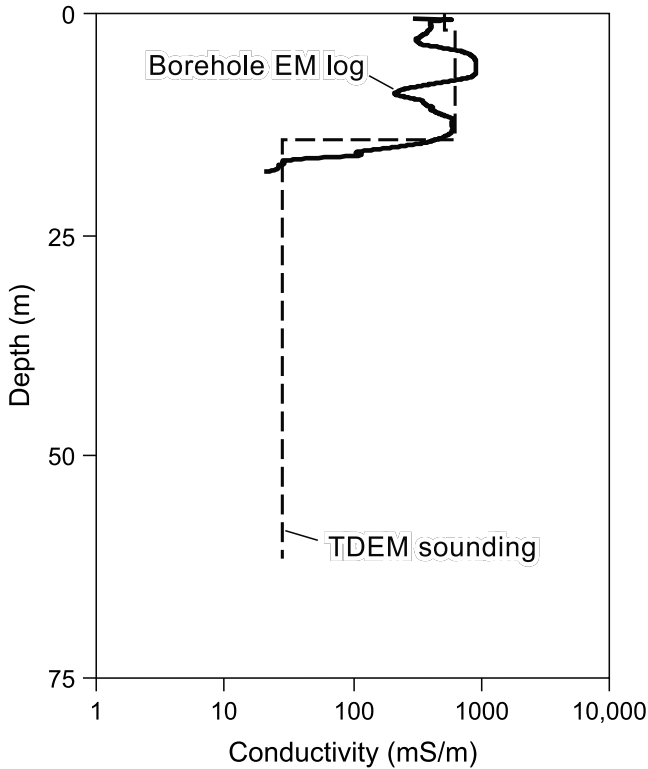


Figure 4. Comparison of conductivity profiles acquired at a monitoring well using a borehole induction instrument and adjacent to the well using a time domain electromagnetic induction (TDEM) instrument (TDEM site 1, Figure 2).

1 ms) and high apparent resistivities (more than 10 ohm-m resistivity or less than 100 mS m⁻¹ conductivity), whereas transients measured over the saline-water plume have longer durations (more than 1 ms) and lower minimum apparent resistivities (a few ohm-m resistivity or a few hundred millisiemens per meter conductivity). Coherent increases in apparent resistivity observed at late times in transients acquired over the saline-water plume confirm that the soundings reached nonsalinized strata beneath the plume (Figure 5). Three- to five-layer models produced synthetic transients that fit the transients observed at each site to better than 3 percent difference between the actual and synthetic transients. The model that fits the transient acquired at TDEM site 5 in the northwestern branch of the plume (Figures 2 and 5) indicates the presence of conductive ground (less than 10 ohm-m resistivity or more than 100 mS m⁻¹ conductivity) from the surface to a depth of about 23 m; the most conductive zone (1 ohm-m resistivity or 1000 mS m⁻¹ conductivity) is between 5 and 23 m depth.

[16] Despite different instrument types, assumptions, and processing algorithms, cross sections constructed from TDEM soundings agree well with apparent conductivity maps constructed from airborne data. Where apparent conductivity maps show elevated values, TDEM soundings indicate conductive layers in the near surface. Where apparent conductivity maps show low values, TDEM soundings indicate resistive layers in the near surface. Section A-A', constructed from best fit conductivity models for soundings acquired along the main axis of the saline-

water plume (Figures 2 and 6), illustrates that moderately conductive (100–300 mS m⁻¹) and highly conductive (300–1000 mS m⁻¹) layers are thickest beneath the oil field on the Permian upland (33–38 m thick at soundings 18 and 17), further suggesting an oil field source for the plume. These layers thin northward (toward the Red River) across the Pleistocene terrace from 15 m at sounding 1 to 7 m at sounding 13 and are not present at sounding 4. Modeled conductivities of 10–100 mS m⁻¹ in layers underlying the conductive layers are similar to apparent values measured beneath the plume using borehole instruments and beyond the boundaries of the saline-water plume using airborne and ground-based induction coils.

[17] The relative merits of borehole induction logs and surface TDEM soundings are evident when we compare an induction log acquired at a monitoring well with the best fit conductivity model obtained from a TDEM sounding acquired adjacent to the well (Figure 4). The borehole log clearly shows the base of the saline-water plume and stratigraphic detail, allows us to determine which stratal units have been infiltrated by saline water, can guide water sampling, and allows us to associate chloride content in water to measured ground conductivity. TDEM soundings locate the base of the plume relatively well, produce a good general fit to measured borehole conductivities, are non-invasive, and are more easily acquired than borehole logs, although their vertical resolution is poor. TDEM soundings also explore deeply enough to allow us to determine optimal drilling depths and to ensure that the boreholes reached the base of the saline-water plume.

4. Determining Plume Volume

[18] Once the apparent conductivity range has been established for salinized and nonsalinized ground, EM data can be used to estimate the subsurface volume infiltrated by

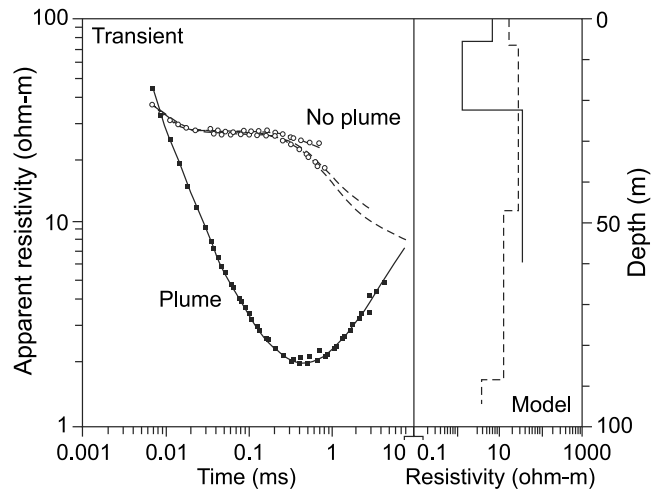


Figure 5. Comparison of transient signals (left) and best fit conductivity models (right) from TDEM soundings acquired over the saline-water plume (TDEM site 5, Figure 2) and in a nonplume area (TDEM site 3). Solid and open symbols at left are the observed transients. Solid and dashed lines at left are the synthetic transients calculated using the models shown at right.

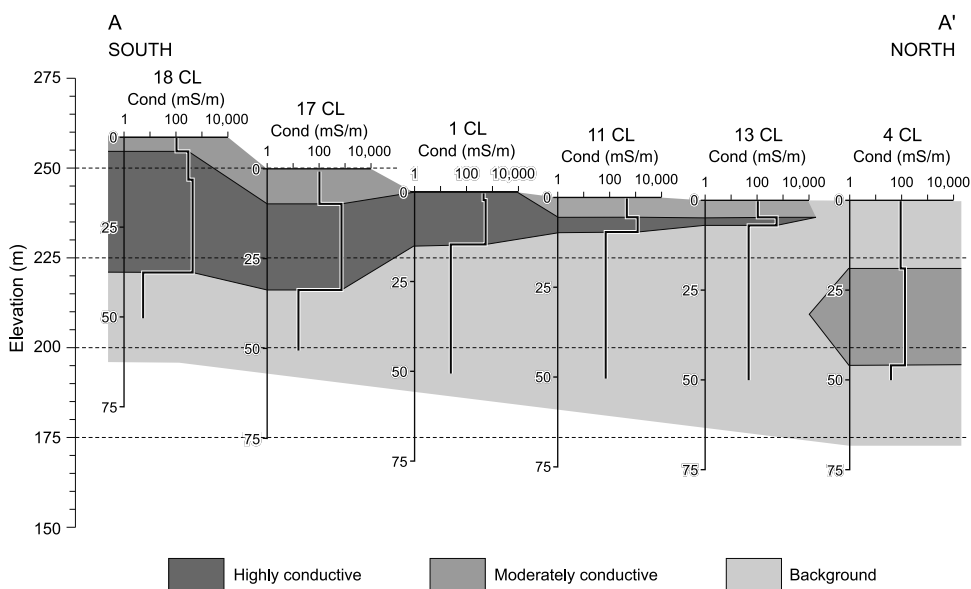


Figure 6. TDEM cross section A-A' along main axis of the saline-water plume (Figure 2) showing land-surface elevations and elevations and conductivities of the modeled layers. Highly conductive layers have conductivities greater than 300 mS m⁻¹, moderately conductive layers have conductivities between 100 and 300 mS m⁻¹, and background layers have conductivities less than 100 mS m⁻¹.

saline water. Areal salinization extent for a given airborne coil frequency can be determined by gridding the apparent conductivity measurements and calculating the total surface area having values above a given threshold, which is about 70 mS m⁻¹ for the study area but will vary elsewhere because of regional differences in soil type, rock type, water saturation, water chemistry, and layer geometry. Excluding unrelated, highly conductive ground near the Red River, the total salinized area considered to be within the plume (ground having conductivities above 70 mS m⁻¹) is about 10 km². This value, including 3.1 km² on the Permian upland and 6.9 km² on the Pleistocene terrace, is about 45 times the size of the barren area mapped on the ground and on infrared aerial photographs [Hovorka et al., 1999a]. Areas can be calculated similarly for higher conductivity thresholds, producing an areal distribution of salinization intensity.

[19] Plume thickness can be estimated by inverting multi-frequency airborne data if the plume extends no deeper than the exploration depth of the instrument, but more accurate values are obtained using TDEM soundings and borehole data. By multiplying the upland and terrace plume areas (determined from airborne EM data) by average plume thicknesses of 32 m on the upland and 14 m on the terrace (determined from TDEM and borehole data only), we estimate that the total subsurface volume infiltrated by saline water is 193 × 10⁶ m³.

5. Estimating Chloride Mass

[20] Chemical analyses of 40 water samples taken from monitoring wells in the study area reveal a strong empirical relationship between TDS and measured electrical conductivity of the water samples [Hovorka et al., 1999a] and between chloride concentration and measured water conductivity (Figure 7). Borehole measurements using an EM instrument verify that apparent ground conductivity

increases with increasing chloride (and thus TDS) concentration (Figure 8). Chloride concentrations in analyzed samples range from 19 mg L⁻¹ to 44.2 g L⁻¹; measured conductivities for these samples increase from 65 to 10,220 mS m⁻¹. Over this concentration range, the ratio of chloride concentration to measured conductivity increases with chloride concentration, averaging an increase of 3.42 mg L⁻¹ of chloride for every 1 mS m⁻¹ increase in measured conductivity for the most commonly observed chloride concentrations. Recast to equivalent units, this ratio becomes 3.42 g m⁻² mS⁻¹. We can use this ratio to estimate total chloride mass within the exploration range of the airborne induction coils by estimating the apparent electrical conductance of the plume (exploration depth multiplied by apparent conductivity) and recognizing that it is dominantly the dissolved solids that contribute to the anomalously high

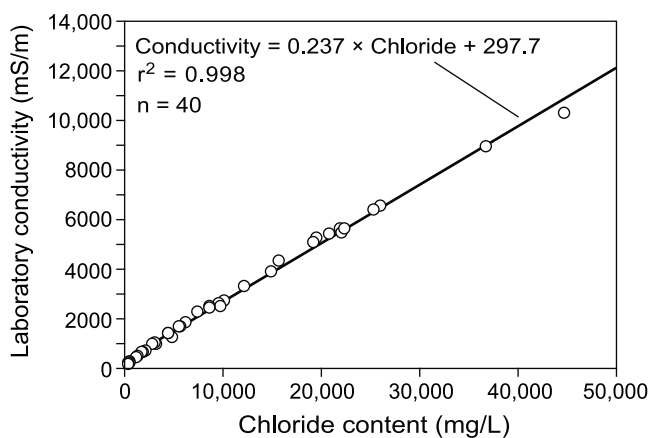


Figure 7. Relationship between chloride content and measured electrical conductivity of water samples from survey-area wells.

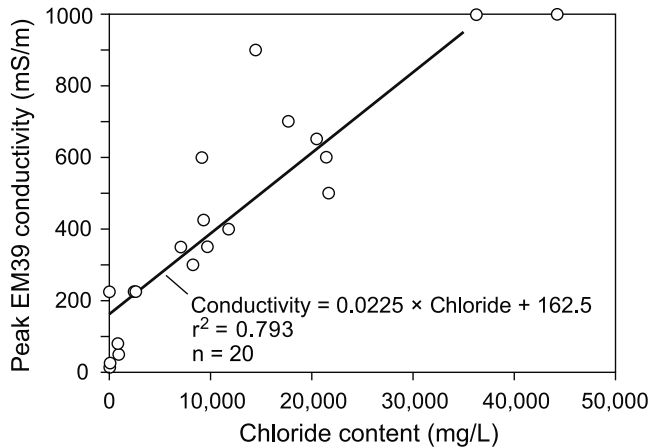


Figure 8. Relationship between chloride content of water samples and peak electrical conductivity measured using a borehole induction logger at the depth of the water sample.

ground conductivities. Once we know the relationship between chloride concentration and conductivity, we can estimate chloride mass within a subsurface volume by measuring ground conductivity, removing the formation or “background” contribution (conductivity in nonplume areas), ascribing all remaining or “excess” conductivity to electrolytic flow of dissolved constituents, and determining the ionic mass required within the exploration depth range to elevate ground conductivity to the measured value.

[21] If we assume that apparent ground conductivity in excess of observed background values of 50 mS m^{-1} is due to the presence of chloride and other ions in pore fluid (i.e., that conductivity is dominantly electrolytic within the plume), we can calculate a mass of chloride per unit area from the empirical chloride:conductivity ratio and a ground conductivity measurement. This number will represent total mass of chloride (but not its concentration because of the electrical equivalence of thin, highly conductive zones and thick, less conductive zones) within the exploration range of a given coil frequency. Total chloride mass will be higher for a given ground conductivity as the EM frequency decreases and exploration depth increases. To estimate chloride mass per unit area for a given apparent conductivity and coil frequency, we (1) calculate how much the conductivity of pore water increases as chloride concentration increases (the chloride:conductivity ratio in $\text{g m}^{-2} \text{ mS}^{-1}$); (2) measure the apparent ground conductivity; (3) determine the exploration depth for the conductivity measurement; (4) subtract the background conductivity from the measured ground conductivity to calculate excess conductivity; (5) multiply the excess conductivity (in mS m^{-1}) by the exploration depth to determine excess conductance (in mS) attributed to saline water; and (6) multiply the excess conductance (in mS) by the chloride:conductivity ratio (in $\text{g m}^{-2} \text{ mS}^{-1}$) to arrive at a chloride mass per unit area. This is the chloride mass associated with the TDS increase required to account for the excess conductance.

[22] To illustrate and verify this approach, we calculated chloride mass for an area near a monitoring well at TDEM site 1 (Figure 2) where we also independently calculated chloride mass from borehole data. From airborne EM data

we know that the apparent conductivity measured by the 900 Hz airborne induction coils at the monitoring well is 325 mS m^{-1} . Removing the background conductivity of 50 mS m^{-1} , there remains 275 mS m^{-1} of excess apparent conductivity that we attribute to electrolytic conductance associated with the presence of chloride and other ionic constituents within the exploration depth range of the instrument. At 325 mS m^{-1} and 900 Hz, the exploration depth is about 30 m (Figure 3). Excess conductance (conductivity multiplied by depth) is thus $275 \text{ mS m}^{-1} \times 30 \text{ m}$, or 8250 mS. Using the restated chloride:conductivity ratio, we calculate the chloride mass per unit area to be $3.42 \text{ g m}^{-2} \text{ mS}^{-1} \times 8250 \text{ mS}$, or 28.2 kg m^{-2} for the 900 Hz airborne data acquired at the monitoring well.

[23] At the same site, we know from water samples and borehole EM logs that (1) saline water has infiltrated coarse sediments that are about 5.4 m thick and (2) the average chloride concentration of water samples from this well is $17,960 \text{ mg L}^{-1}$ [Hovorka et al., 1999a]. Per square meter at the surface, saline water has infiltrated a volume of 5.4 m^3 (5400 L). We do not know the porosity of the sediments beneath the Pleistocene terrace, but we can estimate porosity by dividing the chloride mass calculated from the airborne measurements for one square meter (28.2 kg) by the chloride concentration of the water samples (17.96 g L^{-1}), yielding a water volume of 1570 L. Dividing this number by the infiltrated volume of 5400 L yields a porosity estimate of 29 percent, a low but reasonable value for unconsolidated sand and gravel [Davis, 1969]. Using a higher porosity would increase the water volume and the chloride mass, suggesting that the calculation from airborne EM data slightly underestimates the actual chloride mass. Nevertheless, the reasonableness of this porosity value suggests that the chloride mass estimated using airborne measurements is close to the actual chloride mass at the monitoring well. It would be difficult to improve the accuracy of airborne determinations of chloride mass because (1) the airborne coils respond unequally to similar chloride concentrations at different depths within the exploration range; (2) there are conductivity variations related to lateral and vertical sediment and rock-type changes that are ignored in these calculations; (3) there are conductivity variations caused by chloride in the unsaturated zone and in fine-grained units that violate the electrolytic assumption; and (4) exploration depth may be greater or less than the skin depth, depending on the actual conductivity profile. Despite vertical resolution shortcomings that we avoided by using borehole and TDEM measurements to establish salinization depth, depth inversions of airborne EM data might yield apparent conductivity profiles that are closer to true subsurface conductivity and potentially improve the accuracy of chloride mass estimates.

[24] We can calculate chloride mass per unit area for the range of observed conductivities for the 900, 7200, and 56,000 Hz airborne coils (Figure 9) in a manner similar to that used at the monitoring well. To estimate total chloride mass within the exploration range of a given coil frequency, we must determine the incremental areas having a given conductivity range, multiply those areas by the chloride mass per unit area value for that conductivity and frequency, and then add each mass value to all others for that coil frequency (Figure 10).

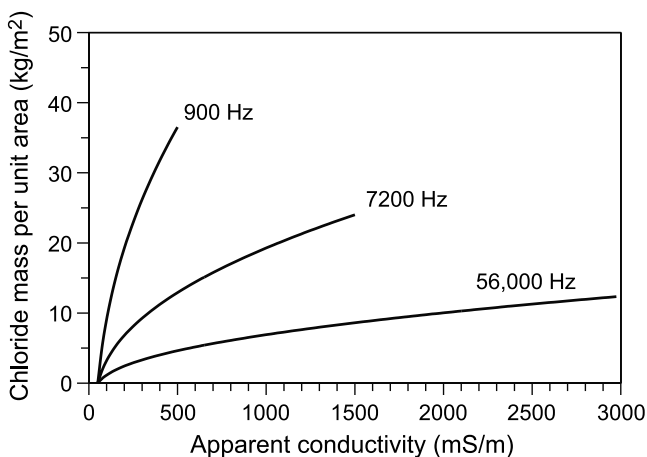


Figure 9. Above-background chloride mass per unit area calculated for 900, 7200, and 56,000 Hz airborne coils assuming background conductivity values of 50 mS m^{-1} and a chloride:conductivity ratio of $3.42 \text{ g m}^{-2} \text{ mS}^{-1}$.

[25] Because lower frequencies have greater exploration depths (and higher chloride mass per unit area values) for a given ground conductivity, the choice of coil frequency for chloride mass calculations is important. TDEM soundings show that conductive ground reaches maximum depths of 7–43 m, which are beyond the exploration depth of the 56,000 Hz and, to a lesser extent, the 7200 Hz coils when operating over conductive ground. Chloride mass estimates made at these frequencies will be lower than those made from 900 Hz data and will underestimate total chloride mass, but they may reveal useful information about vertical distribution of chloride. Calculations made from the 900 Hz data indicate that total chloride mass in the saline-water plume is about $1.5 \times 10^8 \text{ kg}$. This chloride mass is equivalent to the amount of chloride contained in $2.3 \times 10^9 \text{ L}$ (14×10^6 barrels (bbl)) of

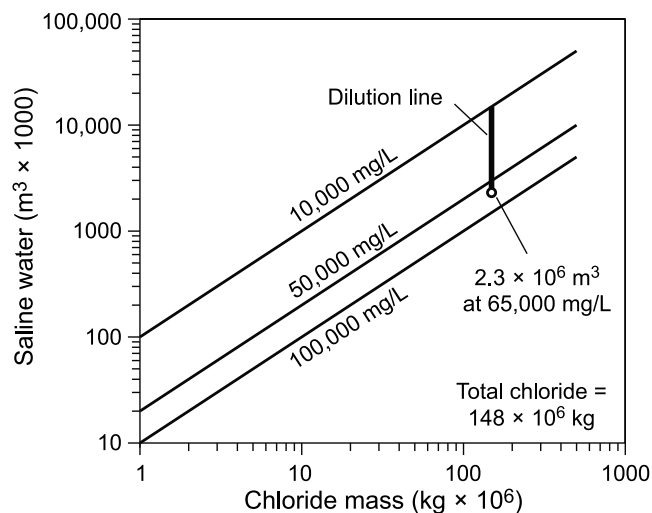


Figure 11. Estimated volume of original brine (at $65,000 \text{ mg L}^{-1}$ chloride concentration) within the saline-water plume and equivalent volumes of saline water at diluted chloride concentrations.

saline water with a concentration of $65,000 \text{ mg L}^{-1}$, the approximate value of brine produced in the nearby oil field (Figure 11). Chloride concentrations have been diluted from original concentrations to the wide range of values observed in monitoring wells, increasing the total volume of saline water within the plume to more than $16 \times 10^9 \text{ L}$ (100×10^6 bbl).

6. Other Constituents

[26] At this site, chloride was the dominant anion in the electrolyte and was the constituent of greatest concern in nearby water wells and surface water bodies. We were able to estimate chloride mass per unit area and total mass from

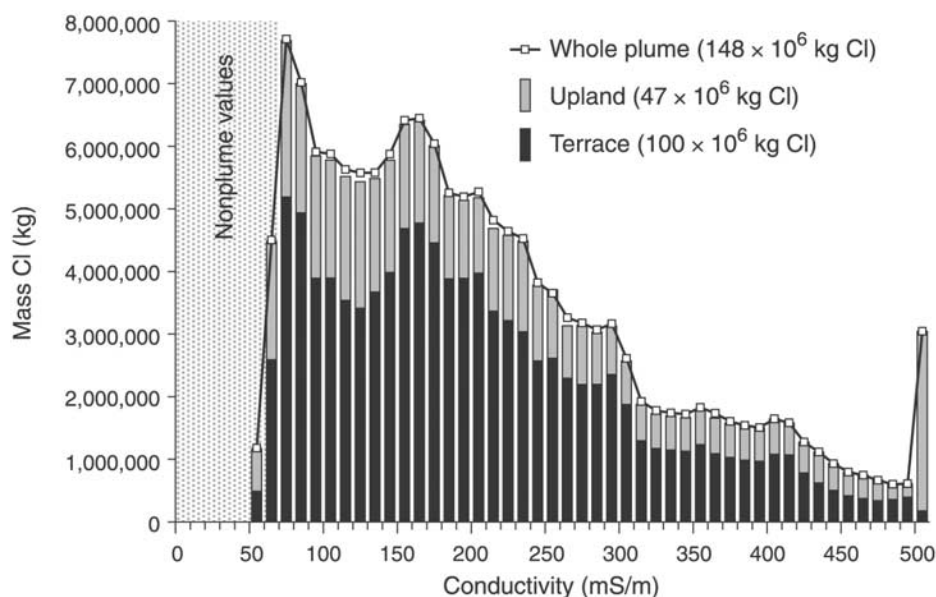


Figure 10. Estimates of chloride mass within apparent conductivity ranges measured by the 900 Hz airborne induction coils. Values below 70 mS m^{-1} are outside the saline-water plume.

ground conductivities measured by the airborne instrument because (1) electrolytic (as opposed to formation) effects dominated ground conductivity within the plume, (2) there was a linear relationship between chloride and TDS concentrations evident from chemical analyses of water samples from the saline-water plume, (3) ground conductivity in this area increases linearly with TDS concentration of pore water in this concentration range, and (4) exploration depth of the airborne instrument was sufficient to penetrate the plume entirely. By extension, the same approach could be used to estimate TDS mass per unit area and total mass or, indeed, the mass per unit area and total mass of any ionic constituent in the electrolyte that varies linearly with TDS (not all do), as long as electrolytic conductance is the dominant control on ground conductivity. The electrolytic dominance and the linear relationships among TDS and ionic constituents of interest can be confirmed by chemically analyzing water samples of varying TDS concentration and comparing the results to borehole conductivity measurements.

7. Conclusions

[27] Ground-based EM methods can be used to establish saline-water plume extent over relatively small areas (up to a few square kilometers) and are needed to determine salinization boundaries and conductivity ranges for airborne surveys, which are best suited for areas larger than a few square kilometers. Airborne surveys allow investigators to screen large areas rapidly, identify salinized areas, quantify the areal extent and intensity of salinization, locate potential salinity sources, determine optimal borehole and follow-up geophysical survey locations, and estimate the total mass of chloride (or other ionic constituents that covary with TDS) within the exploration depth range of a given coil frequency.

[28] TDEM soundings complement airborne data by detecting the top and bottom of a saline-water plume, extending the exploration depth below the deepest levels investigated using airborne EM, and revealing averaged conductivity values of subsurface materials. TDEM soundings can also help anticipate required drilling depths and can serve as rapid, noninvasive, and low-cost borehole proxies where drilling is impractical or impossible.

[29] Borehole induction logs most accurately determine the vertical extent of salinization, identify strata carrying saline water, confirm the relationship between ground conductivity and ionic concentration, and verify that current flow within the plume is dominantly electrolytic. Once the relationship between an ionic constituent and conductivity is established, total mass of the ionic constituent can be estimated from airborne EM data. Total mass and total infiltrated volume calculated from geophysical and geochemical data are critical values to be considered when assessing salinization impact and considering remediation options.

[30] **Acknowledgments.** This study was funded by the Railroad Commission of Texas (RRC), A. R. Dutton, Principal Investigator. Interpretations and conclusions presented in this paper are not necessarily those of the RRC. RRC staff Fred McNeel and Ray Horton facilitated land access and provided historical records and water analyses. Foxhollow Consultants provided access to monitoring wells. M. U. Blüm assisted with the acquisition of geophysical data. A. R. Dutton, S. D. Hovorka, Matthew Mahoney, Robin Nava, and E. J. Sullivan conducted borehole drilling and

logging and water sampling. Bruce D. Smith and two anonymous reviewers provided numerous helpful suggestions that improved the accuracy and clarity of the manuscript.

References

- Banerjee, S., D. K. Das, B. R. Yadav, N. Gupta, H. Chandrasekharan, A. K. Ganjoo, and R. Singh, Estimation of soil salinity at IARA farm by inductive electromagnetic technique, *J. Indian Soc. Soil Sci.*, 46(1), 110–115, 1998.
- Banin, A., and A. Fish, Secondary desertification due to salinization of intensively irrigated lands: The Israeli experience, *Environ. Monit. Assess.*, 37, 17–37, 1995.
- Barica, J., Salinization of groundwater in arid zones, *Water Res.*, 6, 925–933, 1972.
- Chen, H., Y. Zhang, X. Wang, Z. Ren, and L. Li, Salt-water intrusion in the lower reaches of the Weihe River, Shandong Province, China, *Hydrogeol. J.*, 5(3), 82–88, 1997.
- Corwin, D. L., and J. D. Rhoades, An improved technique for determining soil electrical conductivity-depth relations from above-ground electromagnetic measurements, *Soil Sci. Soc. Am. J.*, 46, 517–520, 1982.
- Corwin, D. L., and J. D. Rhoades, Measurement of inverted electrical conductivity profiles using electromagnetic induction, *Soil Sci. Soc. Am. J.*, 48, 288–291, 1984.
- Davis, S. N., Porosity and permeability of natural materials, in *Flow Through Porous Media*, edited by R. J. M. De Wiest, pp. 54–89, Academic, San Diego, Calif., 1969.
- De Jong, E., A. K. Ballantyne, D. R. Cameron, and D. W. L. Read, Measurement of apparent electrical conductivity of soils by an electromagnetic induction probe to aid salinity surveys, *Soil Sci. Soc. Am. J.*, 43, 810–812, 1979.
- Dutton, A. R., B. C. Richter, and C. W. Kreidler, Brine discharge and salinization, Concho River watershed, west Texas, *Ground Water*, 27(3), 375–383, 1989.
- Dwivedi, R. S., K. Sreenivas, and K. V. Ramana, Inventory of salt-affected soils and waterlogged areas: A remote sensing approach, *Int. J. Remote Sens.*, 20(8), 1589–1599, 1999.
- Enfield, C. G., and D. D. Evans, Conductivity instrumentation for in situ measurement of soil salinity, *Soil Sci. Soc. Am. J.*, 33, 787–791, 1969.
- Frischknecht, F. C., V. F. Labson, B. R. Spies, and W. L. Anderson, Profiling using small sources, in *Electromagnetic Methods in Applied Geophysics: Applications, Part A and Part B*, edited by M. N. Nabighian, pp. 105–270, Soc. of Explor. Geophys., Tulsa, Okla., 1991.
- Funakawa, S., R. Suzuki, E. Karbozova, T. Kosaki, and N. Ishida, Salt-affected soils under rice-based irrigation agriculture in southern Kazakhstan, *Geoderma*, 97, 61–85, 2000.
- Ghassemi, F., A. J. Jakeman, and H. A. Nix, *Salinization of Land and Water Resources*, 526 pp., CAB Int., Wallingford, U.K., 1995.
- Gilboa, Y., The salinization in the alluvial aquifers of the coast of Peru, *Bol. Soc. Geol. Peru*, 57/58, 35–58, 1977.
- Halvorson, A. D., and J. D. Rhoades, Assessing soil salinity and identifying potential saline-seep areas with field soil resistance measurements, *Soil Sci. Soc. Am. J.*, 38, 576–581, 1974.
- Hem, J. D., Study and interpretation of the chemical characteristics of natural water, *U.S. Geol. Surv. Prof. Pap.*, 2254, 263 pp., 1985.
- Hendry, M. J., and G. D. Buckland, Causes of soil salinization, 1, A basin in southern Alberta, Canada, *Ground Water*, 28(3), 385–393, 1990.
- Hillman, R. M., Land and stream salinity in western Australia, in *Land and Stream Salinity: Developments in Agricultural Engineering*, vol. 2, edited by J. W. Holmes and T. Talsma, pp. 11–18, Elsevier Sci., New York, 1981.
- Hovorka, S. D., A. R. Dutton, J. G. Paine, R. Nava, and M. Blüm, Site investigation of the Montague Salt-Water Seep, Montague County, Texas (RRC Cleanup No. 09-50211), contract report, 133 pp., Bur. of Econ. Geol., Univ. of Tex. at Austin, 1999a.
- Hovorka, S. D., J. G. Paine, and A. R. Dutton, Permeability structure of a north Texas Permian fluvial and Quaternary terrace system delimited by saline plumes, in *American Association of Petroleum Geologists Annual Convention Program*, p. A63, Am. Assoc. of Petrol. Geol., Tulsa, Okla., 1999b.
- Johnston, R., and J. Kamprad, Application of Landsat thematic mapping to geology and salinity in the Murray Basin, *BMR J. Aust. Geol. Geophys.*, 11(3), 363–366, 1988.
- Kaufman, A. A., and G. V. Keller, *Frequency and Transient Soundings: Methods in Geochemistry and Geophysics*, vol. 16, 685 pp., Elsevier Sci., New York, 1983.

- Kirchner, J., J. H. Moolman, and A. G. Reynders, Causes and management of salinity in the Breede River valley, South Africa, *Hydrogeol. J.*, 5(1), 98–108, 1997.
- Kovda, V. A., *Origin and Regime of Saline Soils*, 509 pp., Akad. Nauk, Moscow, 1946.
- Lesch, S. M., D. J. Strauss, and J. D. Rhoades, Spatial prediction of soil salinity using electromagnetic induction techniques, 1, Statistical prediction models: A comparison of multiple linear regression and cokriging, *Water Resour. Res.*, 31(2), 373–386, 1995.
- Lesch, S. M., J. Herrero, and J. D. Rhoades, Monitoring for temporal changes in soil salinity using electromagnetic induction techniques, *Soil Sci. Soc. Am. J.*, 62, 232–242, 1998.
- Macumber, P. G., Interrelationship between physiography, hydrology, sedimentation, and salinization of the Loddon River Plains, Australia, *J. Hydrol.*, 7, 39–57, 1969.
- Marie, A., and A. Vengosh, Sources of salinity in ground water from Jericho area, Jordan Valley, *Ground Water*, 39(2), 240–248, 2001.
- McKenzie, R. C., R. J. George, S. A. Woods, M. E. Cannon, and D. L. Bennett, Use of the electromagnetic-induction meter (EM38) as a tool in managing salinisation, *Hydrogeol. J.*, 5(1), 37–50, 1997.
- McNeill, J. D., Electrical conductivity of soils and rocks, *Tech. Note TN-5*, 22 pp., Geonics Ltd., Mississauga, Ont., Canada, 1980a.
- McNeill, J. D., Electromagnetic terrain conductivity measurement at low induction numbers, *Tech. Note TN-6*, 15 pp., Geonics Ltd., Mississauga, Ont., Canada, 1980b.
- Miller, M. R., P. L. Brown, J. J. Donovan, R. N. Bergatino, J. L. Sonderegger, and F. A. Schmidt, Saline seep development and control in the North American Great Plains-Hydrogeological aspects, in *Land and Stream Salinity: Developments in Agricultural Engineering*, vol. 2, edited by J. W. Holmes and T. Talsma, pp. 115–141, Elsevier Sci., New York, 1981.
- Nightingale, H. I., Soil and ground-water salinization beneath diversified irrigated agriculture, *Soil Sci.*, 118(6), 365–373, 1974.
- Paine, J. G., A. R. Dutton, J. S. Mayorga, and G. P. Saunders, Identifying oil-field salinity sources with airborne and ground-based geophysics: A west Texas example, *Leading Edge*, 16(11), 1603–1607, 1997.
- Paine, J. G., A. R. Dutton, and M. U. Blüm, Using airborne geophysics to identify salinization in west Texas, *Rep. of Invest.*, 257, 69 pp., Bur. of Econ. Geol., Univ. of Tex. at Austin, 1999.
- Pankova, E. I., and D. I. Rukhovich, Monitoring of salinization of irrigated soils in arid regions by remote sensing methods, *Eurasian Soil Sci.*, 32(2), 225–235, 1999.
- Parasnis, D. S., *Mining Geophysics*, 395 pp., Elsevier Sci., New York, 1973.
- Prakash, V. A., and D. K. Chadha, Genetic causes of salinization of ground-water in Haryana, India, *Bull. Indian Geol. Assoc.*, 16(1), 99, 1983.
- Red River Authority of Texas, Regional assessment of water quality, Red River basin of Texas, third biennial report, prepared in cooperation with the Tex. Nat. Resour. Conserv. Comm., 220 pp., Wichita Falls, 1996.
- Rhoades, J. D., and D. L. Corwin, Determining soil electrical conductivity-depth relations using an inductive electromagnetic soil conductivity meter, *Soil Sci. Soc. Am. J.*, 45, 255–260, 1981.
- Richter, B. C., and C. W. Kreitler, *Geochemical Techniques for Identifying Sources of Ground-Water Salinization*, edited by K. C. Smoley, 258 pp., CRC Press, Boca Raton, Fla., 1993.
- Richter, B. C., A. R. Dutton, and C. W. Kreitler, Identification of sources and mechanisms of salt-water pollution affecting ground-water quality: A case study, west Texas, *Rep. of Invest.*, 191, 43 pp., Bur. of Econ. Geol., Univ. of Tex. at Austin, 1990.
- Rosenthal, E., A. Vinokurov, D. Ronen, M. Magaritz, and S. Moshkovitz, Anthropogenically induced salinization of groundwater: A case study from the Coastal Plain aquifer of Israel, *J. Contam. Hydrol.*, 11, 149–171, 1992.
- Schofield, N. J., and J. K. Ruprecht, Regional analysis of stream salinisation in southwest Western Australia, *J. Hydrogeol.*, 112, 19–39, 1989.
- Smith, B. D., R. Bisdorf, L. J. Slack, and A. T. Mazzella, Evaluation of electromagnetic mapping methods to delineate subsurface saline waters in the Brookhaven oil field, Mississippi, in *Proceedings of the Symposium on the Application of Geophysics to Engineering and Environmental Problems*, compiled by R. S. Bell, pp. 685–693, Environ. and Eng. Geophys. Soc., Wheat Ridge, Colo., 1997.
- Smith, D. R., Salinization in Uzbekistan, *Post-Soviet Geogr.*, 33, 21–33, 1992.
- Spies, B. R., and F. C. Frischknecht, Electromagnetic sounding, in *Electromagnetic Methods in Applied Geophysics: Applications, Part A and Part B*, edited by M. N. Nabighian, pp. 285–386, Soc. of Explor. Geophys., Tulsa, Okla., 1991.
- Telford, W. M., L. P. Geldart, R. E. Sheriff, and D. A. Keys, *Applied Geophysics*, 860 pp., Cambridge Univ. Press, New York, 1976.
- Valenza, A., J. C. Grillot, and J. Dazy, Influence of groundwater on the degradation of irrigated soils in a semi-arid region, the inner delta of the Niger River, Mali, *Hydrogeol. J.*, 8, 417–429, 2000.
- Vengosh, A., and A. Ben-Zvi, Formation of a salt plume in the Coastal Plain aquifer of Israel: The Be'er Toviyya region, *J. Hydrol.*, 160, 21–52, 1994.
- Wang, B., H. Qiu, Q. Xu, X. Zheng, and G. Liu, The mechanism of ground-water salinization and its control in the Yaoba Oasis, Inner Mongolia, *Acta Geol. Sin.*, 74(2), 362–369, 2000.
- West, G. F., and J. C. Macnae, Physics of the electromagnetic induction exploration method, in *Electromagnetic Methods in Applied Geophysics: Applications, Part A and Part B*, edited by M. N. Nabighian, pp. 5–45, Soc. of Explor. Geophys., Tulsa, Okla., 1991.
- Whittemore, D. O., Geochemical identification of salinity sources, in *Salinity in Watercourses and Reservoirs: Proceedings of the 1983 International Symposium on State-of-the-Art Control of Salinity*, edited by R. H. French, pp. 505–514, Butterworth-Heinemann, Woburn, Mass., 1984.
- Whittemore, D. O., Geochemical differentiation of oil and gas brine from other saltwater sources contaminating water resources: Case studies from Kansas and Oklahoma, *Environ. Geosci.*, 2(1), 15–31, 1995.
- Williams, B. G., and G. C. Baker, An electromagnetic induction technique for reconnaissance surveys of soil salinity hazards, *Aust. J. Soil Res.*, 20, 107–118, 1982.
- Williams, B. G., and M. Braunach, The detection of subsurface salinity within the Northern Slopes region of Victoria, Australia, in *Salinity in Watercourses and Reservoirs: Proceedings of the 1983 International Symposium on State-of-the-Art Control of Salinity*, edited by R. H. French, pp. 515–524, Butterworth-Heinemann, Woburn, Mass., 1984.
- Williams, B. G., and F.-T. Fidler, The use of electromagnetic induction for locating subsurface saline material, in *Relation of Groundwater Quantity and Quality*, edited by F. X. Dunin, *IAHS Publ.*, 146, 189–196, 1985.

J. G. Paine, Bureau of Economic Geology, University of Texas at Austin, University Station, Box X, Austin, TX 78713-8924, USA. (jeff.paine@beg.utexas.edu)